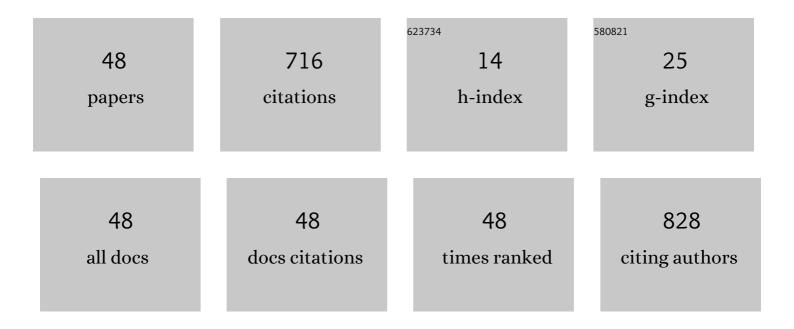
## Siqing Liu

List of Publications by Year in descending order

Source: https://exaly.com/author-pdf/3878292/publications.pdf Version: 2024-02-01



SIGING LIU

#	Article	IF	CITATIONS
1	Midlatitude Plasma Bubbles Over China and Adjacent Areas During a Magnetic Storm on 8 September 2017. Space Weather, 2018, 16, 321-331.	3.7	95
2	Merging of Storm Time Midlatitude Traveling Ionospheric Disturbances and Equatorial Plasma Bubbles. Space Weather, 2019, 17, 285-298.	3.7	58
3	A regional ionospheric TEC mapping technique over China and adjacent areas on the basis of data assimilation. Journal of Geophysical Research: Space Physics, 2015, 120, 5049-5061.	2.4	57
4	Regional $3\hat{a} \in \mathbf{D}$ ionospheric electron density specification on the basis of data assimilation of ground $\hat{a} \in \mathbf{D}$ and radio occultation data. Space Weather, 2016, 14, 433-448.	3.7	43
5	Prediction of the <i>AU</i> , <i>AL</i> , and <i>AE</i> indices using solar wind parameters. Journal of Geophysical Research: Space Physics, 2013, 118, 7683-7694.	2.4	36
6	Contribution of convective transport to stormtime ring current electron injection. Journal of Geophysical Research, 2003, 108, .	3.3	34
7	A New Forecasting Index for Solar Wind Velocity Based on EIT 284 ÃÂObservations. Solar Physics, 2008, 250, 159-170.	2.5	30
8	An Exospheric Temperature Model Based On CHAMP Observations and TIEGCM Simulations. Space Weather, 2018, 16, 147-156.	3.7	29
9	Statistical Analysis of Equatorial Plasma Irregularities Retrieved From Swarm 2013–2019 Observations. Journal of Geophysical Research: Space Physics, 2020, 125, e2019JA027022.	2.4	28
10	Statistical Analysis of the Main Ionospheric Trough Using Swarm in Situ Measurements. Journal of Geophysical Research: Space Physics, 2020, 125, e2019JA027583.	2.4	25
11	lonospheric response to CIRâ€induced recurrent geomagnetic activity during the declining phase of solar cycle 23. Journal of Geophysical Research: Space Physics, 2015, 120, 1394-1418.	2.4	23
12	Quantitative Prediction of Highâ€Energy Electron Integral Flux at Geostationary Orbit Based on Deep Learning. Space Weather, 2018, 16, 903-916.	3.7	22
13	The Interaction between the LEO Satellite Constellation and the Space Debris Environment. Applied Sciences (Switzerland), 2021, 11, 9490.	2.5	18
14	A regional ionospheric TEC mapping technique over China and adjacent areas: GNSS data processing and DINEOF analysis. Science China Information Sciences, 2015, 58, 1-11.	4.3	15
15	An Ionosphere Specification Technique Based on Data Ingestion Algorithm and Empirical Orthogonal Function Analysis Method. Space Weather, 2018, 16, 1410-1423.	3.7	15
16	Ionospheric Response to the 2018 Sudden Stratospheric Warming Event at Middle―and Low‣atitude Stations Over China Sector. Space Weather, 2019, 17, 1230-1240.	3.7	15
17	On energetic electrons (>38 keV) in the central plasma sheet: Data analysis and modeling. Journal of Geophysical Research, 2011, 116, n/a-n/a.	3.3	12
18	Prediction of the smoothed monthly mean sunspot numbers for solar cycle 24. Science in China Series G: Physics, Mechanics and Astronomy, 2008, 51, 1938-1946.	0.2	10

Siqing Liu

#	Article	IF	CITATIONS
19	Statistical analysis and verification of 3â€hourly geomagnetic activity probability predictions. Space Weather, 2015, 13, 831-852.	3.7	10
20	Statistical Study of Magnetic Topology for Eruptive and Confined Solar Flares. Journal of Geophysical Research: Space Physics, 2018, 123, 1704-1714.	2.4	10
21	Generation of ionospheric scintillation maps over Southern China based on Kriging method. Advances in Space Research, 2020, 65, 2808-2820.	2.6	10
22	Operational Space Weather Services in National Space Science Center of Chinese Academy of Sciences. Space Weather, 2015, 13, 599-605.	3.7	9
23	Two empirical models for shortâ€ŧerm forecast of <i>Kp</i> . Space Weather, 2017, 15, 503-516.	3.7	9
24	Statistical study of GNSS L-band solar radio bursts. GPS Solutions, 2018, 22, 1.	4.3	9
25	Forecasting High‣peed Solar Wind Streams Based on Solar Extreme Ultraviolet Images. Space Weather, 2019, 17, 1040-1058.	3.7	9
26	The Deflection of Coronal Mass Ejections by the Ambient Coronal Magnetic Field Configuration. Journal of Geophysical Research: Space Physics, 2020, 125, e2019JA027530.	2.4	9
27	Effect of seed electron injection on chorus-driven acceleration of radiation belt electrons. Science China Technological Sciences, 2013, 56, 492-498.	4.0	6
28	Correlated observations and simulations on the buildup of radiation belt electron fluxes driven by substorm injections and chorus waves. Astrophysics and Space Science, 2015, 355, 245-251.	1.4	6
29	Statistical Analysis of Joule Heating and Thermosphere Response During Geomagnetic Storms of Different Magnitudes. Journal of Geophysical Research: Space Physics, 2020, 125, e2020JA027966.	2.4	6
30	Knowledgeâ€Informed Deep Neural Networks for Solar Flare Forecasting. Space Weather, 2022, 20, .	3.7	6
31	Prediction Model for Solar Energetic Proton Events: Analysis and Verification. Space Weather, 2019, 17, 709-726.	3.7	5
32	Space Weather Related to Solar Eruptions With the ASO-S Mission. Frontiers in Physics, 2020, 8, .	2.1	5
33	Latitudinal Impacts of Joule Heating on the High‣atitude Thermospheric Density Enhancement During Geomagnetic Storms. Journal of Geophysical Research: Space Physics, 2021, 126, e2020JA028747.	2.4	5
34	The observation and simulation of ionospheric response to CIR/highâ€speed streamsâ€induced geomagnetic activity on 4 April 2005. Radio Science, 2016, 51, 1297-1311.	1.6	4
35	Modeling the Relationship of ≥2 MeV Electron Fluxes at Different Longitudes in Geostationary Orbit by the Machine Learning Method. Remote Sensing, 2021, 13, 3347.	4.0	4
36	Sunlit boundary ionospheric response to the great flare on Oct. 28, 2003. Science Bulletin, 2004, 49, 1570-1574.	1.7	3

Siqing Liu

#	Article	IF	CITATIONS
37	Comparison of energetic electron flux and phase space density in the magnetosheath and in the magnetosphere. Journal of Geophysical Research, 2012, 117, .	3.3	3
38	Atmospheric density determination using high-accuracy satellite GPS data. Science China Technological Sciences, 2018, 61, 204-211.	4.0	3
39	The Distribution Characteristics of GPS Cycle Slip Over the China Mainland and Adjacent Region During the Declining Solar Activity (2015–2018) Period of Solar Cycle 24. Radio Science, 2021, 56, e2020RS007196.	1.6	3
40	Assessing the Kinematic GPS Positioning Performance Under the Effect of Strong Ionospheric Disturbance Over China and Adjacent Areas During the Magnetic Storm. Radio Science, 2022, 57, .	1.6	3
41	Analyzing deflection of multiple Solar Coronal Mass Ejections from the same active region. Advances in Space Research, 2023, 72, 5263-5274.	2.6	3
42	Comparison of a new model with previous models for the low-latitude magnetopause size and shape. Science Bulletin, 2010, 55, 179-187.	1.7	2
43	Verification of SPE probability forecasts at the Space Environment Prediction Center (SEPC). Science China Earth Sciences, 2016, 59, 1292-1298.	5.2	2
44	Flat-fielding of Full-disk Solar Images with a Gaussian-type Diffuser. Solar Physics, 2019, 294, 1.	2.5	2
45	Using Temporal Relationship of Thermospheric Density With Geomagnetic Activity Indices and Joule Heating as Calibration for NRLMSISEâ€00 During Geomagnetic Storms. Space Weather, 2022, 20, .	3.7	2
46	Cross Calibration of >16 MeV Proton Measurements From NOAA POES and EUMETSAT MetOp Satellites. Journal of Geophysical Research: Space Physics, 2019, 124, 6906-6926.	2.4	1
47	Longâ€Term Variations of >16â€MeV Proton Fluxes: Measurements From NOAA POES and EUMETSAT MetOp Satellites. Journal of Geophysical Research: Space Physics, 2020, 125, e2019JA027635.	2.4	1
48	Impacts of CMEs on Earth Based on Logistic Regression and Recommendation Algorithm. Space: Science & Technology, 2022, 2022, .	2.5	1